Polyamidoamine-drug conjugates containing metal-based anticancer compounds

Aderibigbe B.A.[1*], Mugogodi A.,[1] M. Nwamadi[2] and S.S. Ray[3], V. Steenkamp[4], M. O. Balogun[5], W. M. R. Matshe[5]

[1]Department of Chemistry, Faculty of Science and Agriculture, Alice Campus, University of Fort Hare, South Africa.

[2]Department of Chemistry, Auckland Park Campus, University of Johannesburg, South Africa.

[3]DST/CSIR National Centre for Nanostructured Materials, Council for Scientific and Industrial Research, Pretoria 0001, South Africa

[4]Department of Pharmacology, Faculty of Health Sciences, University of Pretoria, South Africa.

[5]Polymer and Composites, CSIR Materials Science and Manufacturing, Pretoria, South Africa

* **Corresponding author:** blessingaderibigbe@gmail.com

Abstract

Polyamidoamine drug conjugates containing ferrocene and platinum analogues were prepared in this study. Fourier transform infrared spectra confirmed the successful isolation of the conjugates with signals at 3300 cm^{-1} for amide N–H stretch and for C=O stretch at 1655–1635 cm^{-1} resulting from the conjugation of 4-ferrocenylketobutanoic acid. The polyamidoamine drug conjugate particle size was 247.1 nm and 258.3 nm suggesting their ability to exhibit in vitro phagocytosis. The average particle charges were 29 and 30.2, which was indicative of good stability and the capability to resist aggregation. In vitro cytotoxicity studies further revealed that the conjugates **1–5** did not exhibit cytotoxicity towards the normal cell lines (EA.hy926) whereas high cytotoxic activity was noted against the cancer cell lines (MCF-7 and MDA-MB-231) indicating selectivity towards cancer cell lines. Fc-PDA acted as a potentiating agent when incorporated together with DACH $PtCl_2$ in the polymers, resulting in a good inhibitory effect in vitro. However, when combining Fc-PDA with K_2PtCl_4 in the polymer, an antagonistic effect was noted. The current findings implicate that the prepared conjugates hold the potential as therapeutics for the treatment of breast cancer. Further research is required to confirm this.

Keywords: anticancer; cytotoxicity; drug delivery; ferrocene; platinum; polyamidoamine; polymer-conjugate.

1. Introduction

Cancer is one of the leading causes of death worldwide. Of the 8.8 million deaths in 2015, 6% were due to breast cancer [1]. Current breast cancer treatment regimens pose various. One of these being a barrier drug penetration in solid tumours which involves heterogeneous vascular supply and high interstitial pressures within the tumour tissue. Encapsulation of drugs into polymeric carriers may result in improving drug circulation lifetime and hence enhance drug efficacy [2].

The discovery of anticancer drugs containing cisplatin marked a breakthrough for cancer treatment. Cisplatin, cis-diamminedichloroplatinum(II) is currently the most widely used antitumor agent for the treatment of a wide variety of cancers, which includes among others testicular, ovarian, bladder, cervical, breast, head and neck and non-small cell lung cancers [3]. Despite its success, the clinical use of cisplatin is hampered due to the emergence of toxicity such as nephrotoxicity, neurotoxicity, ototoxicity and emetogenesis [4,5,6]. The focus has therefore shifted to the development of second generation anticancer drugs as alternatives, which includes other types of metal-based compounds. To this end ferrocene-based compounds such as ferricenium salts, ferrocene conjugated to biologically active molecules and ferrocenyl compounds coordinated to other metals [7,8,9] have been found to exhibit anticancer properties in various cell lines [8, 10].

In order to further enhance the biological activity of metal-based drugs, some researchers have investigated their efficacy when incorporated into polymeric carriers that act as delivery vehicles. Polyamidoamine (PAA) carriers are classified as synthetic, biodegradable polymers that can be easily prepared by stepwise poly addition of aliphatic amines to bisacrylamides. These carriers contain tertiary amino and amido groups arranged along a backbone in regular sequences [11, 12]. An endless variety of polyamidoamine structures can be synthesized based on the corresponding choice of monomers i.e. functionalized amines and bisacrylamides [11, 13]. Polyamidoamine synthesis is carried out in aprotic solvents and the most commonly used solvents are alcohols and water. Water-soluble polyamidoamines have been extensively researched as anticancer agents by Ferruti and co-workers [12, 14, 15]. Furthermore, polyamidoamine conjugates containing ferrocene derivatives [16] or which originated from neridronic acid [17] have been prepared. Incorporation of these conjugates into polymers has

resulted in reduced toxicity and enhanced intracellular uptake [18,19,20]. Furthermore, by incorporating platinum with selected chemotherapeutic agents such as doxorubicin, paclitaxel, dichloroacetate, curcumin or methotrexate, drug resistance has been overcome **[**21–25].

In the current study, polyamidoamine conjugates containing platinum and, ferrocene derivatives were prepared and characterized using Fourier transform infrared (FTIR) spectroscopy, proton nuclear magnetic resonance spectroscopy (^{1}H NMR), scanning electron microscopy (SEM), transmission electron microscopy (TEM), energy dispersive X-ray (EDX) spectroscopy, particle size analysis and liquid chromatography–mass spectrometry (LC–MS). Drug release studies of the conjugates was performed and in vitro cytotoxicity evaluation of the conjugates against both cancerous and non-cancerous cell lines was performed.

2. Experimental

2.1. Materials

Ferrocene and potassium tetrachloride used to synthesize the platinum and ferrocene analogues were purchased from Merck Chemicals and Sigma Aldrich, respectively. Tetrahydrofuran and dichloromethane were obtained from Merck Chemicals. These solvents were dried over molecular sieves 4 Å (Sigma-Aldrich, South Africa) for 24 h before use. Methylenebisacrylamide (MBA), trimethylamine (DET), 3-dimethylamino-1-propylamine (DEP) (98%), 1,3-propanediamine (PDA), triethylenetriamine (TEA) and 3-diethylaminopropylamine (DMP) were purchased from Sigma-Aldrich. Dialysis of the polymers was carried out using dialysis membranes with molecular cut-off limits of 12,000–14,000 (Sigma-Aldrich).

MCF-7 (HBT-22) and MDA-MB-231 (HBT-26) cell lines were obtained from the American Type Culture Collection (ATCC) and the EA.hy926 cell line was provided as a gift from the University of North Carolina's Lineberger Comprehensive Cancer Centre. Culture medium, saponin, trichloracetic acid, acetic acid, sulforhodamine B (SRB), trypan blue and Tris buffer were procured from Sigma Aldrich (St Louis, USA). Trypsin/EDTA and glutamine were obtained from Gibco (Life technologies)

and foetal calf serum (FCS) from Biochrom (Germany). Phosphate buffered saline (PBS) was purchased from Becton–Dickinson (USA).

2.2. Preparation of platinum and ferrocene analogues

2.2.1. Synthesis of trans cyclohexane-1,2-diamine dichloroplatinum(II) (DACH $PtCl_2$)

Potassium tetrachloroplatinate (1.0 g, 2.41 mmol) was dissolved in 13 mL distilled water followed by the drop-wise addition of trans-1, 2-diaminocyclohexane (DACH) (0.28 mg, 2.41 mmol) during continuous stirring. The resultant mixture was stirred at room temperature overnight, after which it was kept at − 30 °C for 24 h. The precipitate that formed was filtered off and washed with cold water and methanol. The precipitated was then dried in an oven at 40 °C for 6 h [26].

2.2.2. Synthesis of 4-Ferrocenylketobutanoic acid (Fc)

Potassium tetrachloroplatinate (1.0 g, 2.41 mmol) was dissolved in 13 mL distilled water followed by the drop-wise addition of trans-1, 2-diaminocyclohexane (DACH) (0.28 mg, 2.41 mmol) during continuous stirring. The resultant mixture was stirred at room temperature overnight, after which it was kept at − 30 °C for 24 h. The precipitate that formed was filtered off and washed with cold water and methanol. The precipitated was then dried in an oven at 40 °C for 6 h [26].

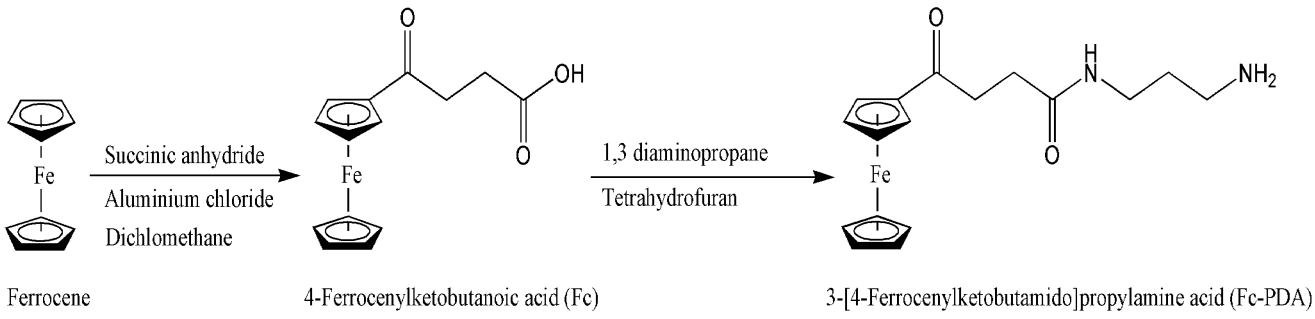

Scheme 1: Reaction scheme for the synthesis of 4-ferrocenylketobutanoic acid (Fc) and 3-[4-ferrocenylketobutamido]propylamine (Fc-PDA)

^{1}H NMR (400 MHz $CDCl_3$-*d6*) δ 2.74 (2H, t, $COCH_2$**CH_2**$COOH$), 3.06 (2H, t, CO**CH_2**CH_2COOH), 4.21 (s, 5H, Cp), 4.5 and 4.8 (s, Cp, 2H each).

2.2.3. Synthesis of 3-[4-ferrocenylketobutamido]propylamine (Fc-PDA)

To a stirred solution of Fc (1.5 g, 5.2 mmol), dissolved in tetrahydrofuran (11 mL), was added N-hydroxysuccinimide (0.60 g, 5.2 mmol) in small portions at room temperature followed by stirring in an ice cold water bath for 15 min. Thereafter N,N'-dicyclohexylcarbodiimide (DCC) (1.08 g, 5.2 mmol) in THF (3 mL) was added drop-wise and stirred for a further 4 h in an ice cold water bath, then at room temperature for 48 h. The solid was filtered off and washed with THF. Thereafter, the filtrate and washings were combined and added drop-wise to a stirred solution of PDA (0.58 g, 7.9 mmol) in THF (14 mL). The reaction was stirred for a further 24 h in an ice cold water bath and then for 6 h at room temperature. The solid that was formed was filtered off and washed with THF. The filtrate and washes were combined and spun to an oily viscous liquid on a rotary evaporator (65 °C bath temperature) (Scheme 1) [27]..

H NMR: δ/ppm 1.9–1.7 (4H, $CH_2\mathbf{CH_2}CH_2$); 2.4–2.2, (4H, Fc-$\mathbf{CH_2}CH_2$ and $NH_2\mathbf{CH_2}$), 2.8–2.9 (2H, $\mathbf{CH_2}CONH_2$), 3.25-3.1 (2H, $CONH\mathbf{CH_2}$); 4.1–4.25 (9H, Cp (Ferrocenyl) [20].

2.3. Reaction procedures for the preparation of carrier and conjugates

2.3.1. Carrier: MBA (500 mg, 3.24 mmol) was dissolved in 20 mL hot distilled water. Upon cooling, DMP (264 mg, 2.59 mmol) and TEA (1 mL) were added and stirred for 6 h, followed by cooling of the reaction in an ice cold water bath and drop-wise addition of PDA (48 mg, 0.65 mmol). The resultant solution was saturated with inert gas and stirred at room temperature for an additional 2 days. The pH of the solution was adjusted to 7 using concentrated HCl. Exhaustive dialysis was performed against water followed by freeze-drying (Yield: 653 mg) (Scheme 2) [29].

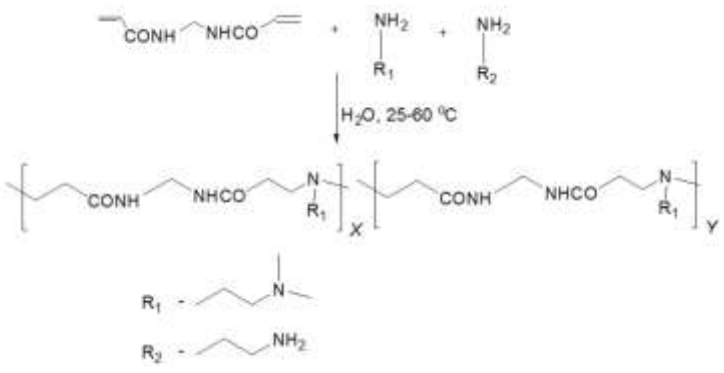

Scheme 2: General reaction equation for the formation of polyamidoamine drug carriers

2.3.2. Conjugate 1: MBA (500 mg, 3.24 mmol) was dissolved in 10 mL of hot distilled water. Upon cooling, DEP (358 mg, 2.75 mmol) was added and stirred for 6 hours at room temperature, followed by dropwise addition of DET (51 mg, 0.49 mmol) in an ice bath. The resultant solution was flushed with argon gas and stirred at room temperature for an additional 3 days. DACH $PtCl_2$ (186 mg, 0.49 mmol) was added to the solution of the carrier protected from light by covering the reaction vessel with alumiuim foil and the pH was adjusted to 5.5. The solution was stirred for a further 3 days with light protection after saturation with inert gas. The resulting solution was stirred at 65°C for 24 hours. The mixture was filtered and exhaustive dialysis was performed followed by freeze-drying (390 mg, 43%) (**Figure 1**).

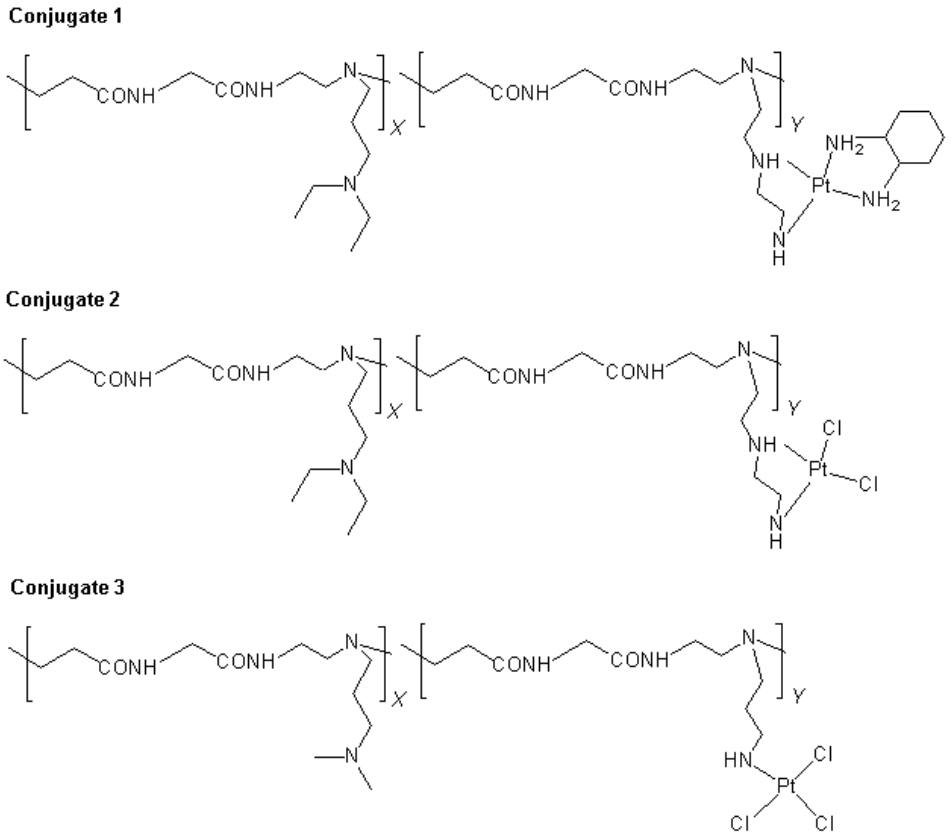

Figure 1: Synthesis of polyamidoamine drug conjugates **1-3**

2.3.3. Conjugate 2: MBA (500 mg, 3.24 mmol) was dissolved in 10 mL of hot distilled water. Upon cooling, DEP (358 mg, 2.75 mmol) was added and stirred for 6 hours, followed by the dropwise addition of DET (51 mg, 0.49 mmol) in an ice bath. The resultant solution was flushed with argon gas and stirred

at room temperature for an additional 3 days. K_2PtCl_4 (203 mg, 0.49 mmol) was added to the solution of the carrier and stirring was continued for a further 24 hours with light protection after saturation with inert gas. The resulting solution was stirred at 45°C for 40 hours and the pH was strictly maintained at 5-6 for the last 0.5 hours. The mixture was filtered and dialysis was performed followed by freeze-drying (491 mg, 54%) (**Figure 1**).

2.3.4. Conjugate 3: The same procedure as for conjugate **2** was followed. MBA (500 mg, 3.24 mmol) in 10 mL water was reacted with DMP (281 mg, 2.75 mmol). The mixture was stirred for 6 h, followed by cooling of the reaction in an ice cold water bath and drop-wise addition of PDA (36 mg, 0.49 mmol). The resultant solution was flushed with argon gas and stirred at room temperature for an additional 3 days. K_2PtCl_4 (203 mg, 0.49 mmol) was added to the solution of the carrier and stirring was continued for a further 24 h under light protection after saturation with inert gas. The conventional work up process was performed followed by freeze drying to isolate water soluble solids (464 mg, 57%) (**Figure 1**).

2.3.5. Conjugate 4: MBA (1000 mg, 6.49 mmol) was dissolved in 20 mL of hot distilled water. Upon cooling, DEP (676 mg, 5.19 mmol) and TEA (1 mL) were added and stirred for 6 hours at room temperature. The resultant solution was protected from light followed by the addition of Fc-PDA (222 mg, 0.649 mmol) dissolved in 2 mL methanol. The solution was flushed with argon gas and stirred at room temperature for an additional 3 days. PDA (48 mg, 0.649 mmol) was then added to the resulting solution followed by stirring for a further 24 hours. The solution was concentrated on a roti evaporator (water bath temperature 60°C) to remove the volatiles and then filtered. Dialysis was performed against water followed by freeze drying and conjugate **3** was isolated (**Figure 2**).

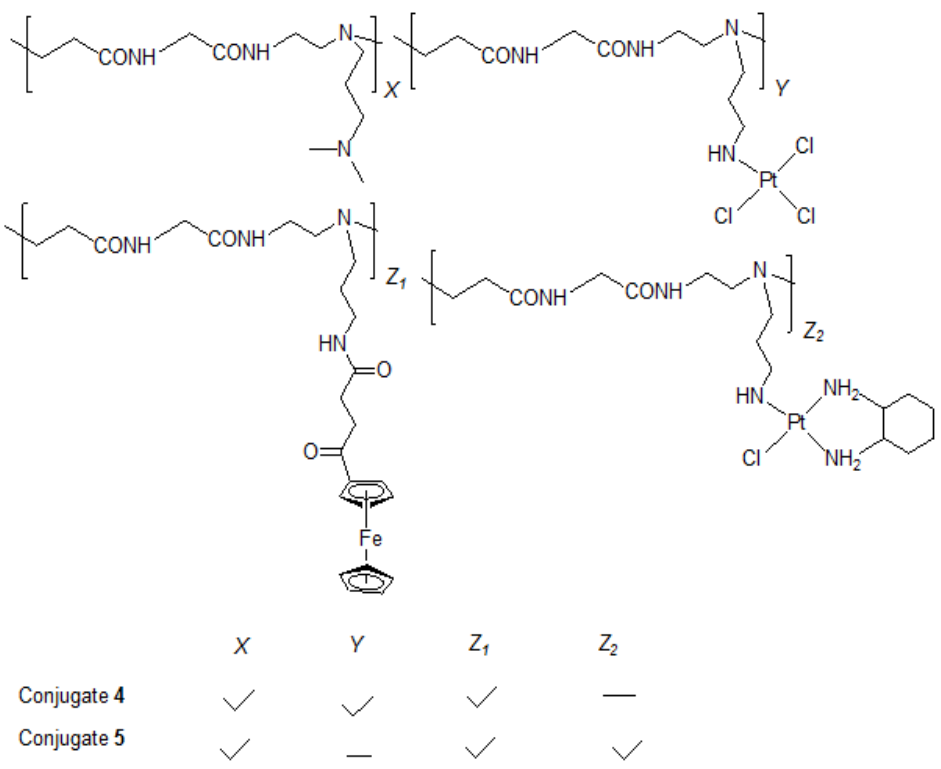

Figure 2: Synthesis of polyamidoamine drug conjugates **4** and **5**

The resultant solid was divided into two portions for preparation of co-conjugates with platinum based drugs. 234 mg of the first portion was dissolved in 7 mL distilled water and protected from light with aluminium foil. K_2PtCl_4 (135 mg, 0.649 mmol) was added to the solution and stirring was continued for a further 24 hours with light protection after saturation with inert gas. The resulting solution was stirred at 45°C for 40 hours and pH was strictly maintained at 5-6 for the last 0.5 hours. The mixture was filtered and dialysis was performed followed by freeze-drying and conjugate **4** was isolated (133 mg, 36%).

2.3.6. Conjugate 5: The second portion of the conjugate (231 mg) as prepared in the procedure described above was dissolved in 7 mL distilled water and protected from light with aluminium foil. 1,2-diaminocyclohexane platinum(II) chloride (DACH $PtCl_2$) (123 mg, 0.649 mmol) was added to the solution, which was protected from light and the pH was adjusted to 5.5. The solution was stirred for a further 3 days under light protection after saturation with inert gas. The resulting solution was stirred at

65 °C for 24 h. The mixture was filtered and dialysis was performed, followed by freeze-drying and conjugate **5** was isolated (112 mg, 31%) (**Figure 2**).

2.4. Characterization techniques

2.4.1. Fourier Transform Infrared Spectroscopy (FTIR): FTIR analysis was carried out on analogues, carriers and drug conjugates within wavenumber range 4000-400 cm^{-1}. FTIR data was obtained by using PerkinElmer Two FTIR spectrometer (USA). The technique was used determine the type of functional groups and to confirm the conjugation of analogues to the polymers.

2.4.2. Proton Nuclear Magnetic Resonance Spectroscopy (^{1}H NMR): ^{1}H NMR was carried out using D_2O in a Varian Unity INOVA 300 MHz Nuclear Magnetic Resonance Spectrometer to elucidate the chemical structure of the analogues, carriers and drug conjugates. The samples for drug conjugates were adjusted to pH 10-11 using sodium hydroxide to get rid of protonation.

2.4.3. Scanning Electron Microscopy (SEM) and Energy Dispersive X-Ray Spectroscopy (EDX): Scanning electron microscopy is an analytical technique useful for obtaining the surface morphology and crystallographic information of a sample. In this study, SEM analysis was performed on JEOL JSM-6390LV scanning electron microscope instrument (Japanese Electron Optical Lab) at an accelerating voltage of 15 kV. All the samples were coated with a thin layer of gold before SEM images were obtained in order to improve the quality of the results. EDX was used to determine elemental composition of polyamidoamine drug conjugates.

2.4.4. Transmission Electron Microscopy (TEM): TEM was used to determine the morphology and to provide an estimation of particle sizes of polyamidoamine drug conjugates. The TEM images were recorded on JEM-1200EX JEOL instrument. Samples of conjugates were dispersed in ethanol before a drop of the solution was deposited onto copper grids and allowed to dry on a filter paper at RT for 15 minutes prior to TEM analysis.

2.4.5. Particle Size Analysis: Particle size analysis was performed using Malvern Zetasizer Nano ZS (Malven Instruments, Worcestershire, UK). Each sample of the conjugate was dissolved in 1 mL of deionized water to form a stock solution. 0.1 mL of the stock solution was diluted to 1 mL with

deionized water, vortexed and filtered through 0.45 μm disc syringe filter. Refractive index of 1.348 and absorption value of 0.001 were used in the determination of the particle sizes of the conjugates and carrier.

2.4.6. Liquid Chromatography Mass Spectrometry (LC-MS)

LC-MS analysis was performed on the polymer-conjugates in order to confirm the formation of the conjugates and the drug conjugation to the polymer. The analysis was performed on conjugates **2** to illustrate the successful conjugation of the drug to the polymer carrier. LC–MS analysis was conducted on a Waters Synapt G2 quadrupole time-of-flight mass spectrometer (Milford, MA, USA). The instrument was connected to a Waters Acquity ultra-performance liquid chromatograph (UPLC) and Acquity photo diode array (PDA) detector. The ionisation was performed with an electrospray source using acone voltage (15 V) and capillary voltage (2.5 kV) and both positive and negative modes were employed. The desolvation gas used was nitrogen gas at 650 l h^{-1} and the temperature of 275 °C. In the analysis, a Waters UPLC BEH C18 column (2.1×100 mm, 1.7 μm particle size) was used and 2 μl was injected for each analysis. The gradient started with 100% using 0.1% (v/v) formic acid (solvent A) and this was kept 100% for 0.5 min, followed by a linear gradient to 22% acetonitrile (solvent B) over 2.5 min, 44% solvent B over 4 min and finally to 100% solvent B over 5 min. The column was subjected to 100% solvent B for an additional 2 min. The column was then re-equilibrated over 1 min to yield a total run time of 15 min. A flow rate of 0.4 mL min^{-1} was applied. Data generated from these runs were subjected to principal component analysis [30].

2.4.7. Drug release studies

Drug release studies was performed on conjugates **2** and **4**. 20 mg of each conjugate was dissolved in 2 mL of distilled water and placed in a dialysis membrane. The membrane was placed in a phosphate buffer solution of either pH 1.2 or 7.4 (simulating gastric pH and blood serum pH, respectively) and dialysis performed using a shaker (Memmert, Germany) maintained at 37 °C. Aliquots (4 mL) were extracted (and replaced by an equal amount of fresh buffer solution) at 40 min time intervals for the first 8 h and then after 24 h periods for the next 5 days. The concentration of drug released was quantified by ultraviolet visible spectroscopy (Fe) and atomic absorption spectroscopy (platinum).

2.4.8. Ultraviolet Visible Spectroscopy (UV/Vis)

Ultraviolet visible spectroscopy was performed using a Perkin Elmer Lambda 365 UV/Vis spectrometer. The maximum absorption wavelength was set at 228 nm for Fc-PDA and it was used for the calibration of the instrument before determining the quantity of ferrocene drug released. A stock solution of 1000 mg/L was prepared and diluted accordingly to form standard solutions of Fc-PDA (100, 10, 1 and 0.1 mg/L) which were used for calibration. The drug concentrations of the samples (released drug) were read at 228 nm. Experiments were conducted in triplicate.

2.4.9. Atomic absorption spectroscopy (AAS)

A Thermo Scientific iCE 3500 Series AA spectrometer was used to determine the concentration of platinum drug. A stock solution of 150 mg/L was prepared and diluted accordingly to form standard solutions of K_2PtCl_4 at concentrations 100, 50, 20 and 5 mg/L which were used for calibration. After calibration of the instrument, aliquots were withdrawn from each sample obtained in the drug release studies and the concentration was recorded. Experiments were conducted in triplicate.

2.4.10. In vitro cytotoxicity evaluation

In vitro cytotoxicity evaluation was performed against breast cancer cell lines (MCF-7 and MDA-MB-231) and normal cell line (EA.hy926). MCF-7 (HBT-22) and MDA-MB-231 (HBT-26) cell lines were obtained from the American Type Culture Collection (ATCC) and the EA.hy926 cell line was provided as a gift from the University of North Carolina's Lineberger Comprehensive Cancer Centre. All cells were maintained in Dulbecco's Modified Essential Medium (DMEM) supplemented with 10% Foetal Calf Serum (FCS) and 2 mM glutamine in 75 mL flasks. The cells were maintained at 37°C in an incubator humidified with an atmosphere of 5% CO_2. When confluent, cells were washed with phosphate buffered saline (PBS) and harvested by detachment using 0.25% trypsin/EDTA. Centrifugation was performed on the detached cells in complete medium at 200 g for 5 minutes. The trypan blue (0.1%) exclusion method was employed to count cell which were diluted to 5 x 104 (MCF-7 and EA.hy926) and 2.5 x 104 (MDA-MB-231) cells/mL 10% FCS medium.

2.4.11. Cytotoxicity assay

Cytotoxicity was evaluated by determination of cell density with sulforhodamine B assay as reported by Vichai and Kirtikara with minor changes [32]. A 100 μL of cell suspension was seeded into a sterile, clear 96-well plates and incubated overnight in an atmosphere of 5% CO_2 at a temperature of 37°C. During incubation, cells were allowed to attach and then exposed to 100 μL of the experimental compounds (0.01 – 100 μM for conjugates, 0.03 – 32 μM for platinum drug). Medium was used as the negative control. Blank and colour controls without cells were included to check for background noise and sterility. The plates were incubated for a period of 72 hours in 5% CO_2 at a temperature of 37°C and then cells were fixed with 50 μL of 50% trichloroacetic acid overnight at 4°C. Fixed cells were washed three times with tap water before staining with 100 μL of 0.057% SRB in 1% acetic acid for 30 minutes. The stained cells were washed four times with 100 μL of 1% acetic acid and then air dried. The bound dye was dissolved using 200 μL Tris-buffer (10mM, pH 10.5). Absorbance was measured on Synergy 2 plate (Bio-tek Instruments, Inc) at 510 nm with reference 630 nm. Assays were carried out using both three intra- and three inter-replicates. Graphpad Prism 5 was used to calculate the IC_{50} values.

3. Results

3.1. FTIR analysis and LC-MS

The FTIR spectrum of 4-Ferrocenylketobutanoic acid revealed peaks for C-H stretch at 2976 cm^{-1}, at 1740 cm^{-1} for C=O stretch for ketone, at 1664 cm^{-1} for C-O stretch for amine and at 1212 cm^{-1} for C-O stretch (**SUPP Figure 1**). The FTIR spectrum of DACH-Pt revealed characteristic peaks at 3260 and 3187 cm^{-1} for N-H stretch for amine and at 2938 and 2863 cm^{-1} for C-H stretch (**SUPP Figure 2**). The FTIR spectra of polyamidoamine drug conjugates **1-5** displayed characteristic absorption peaks (**Figure 3a & b**). The broad peak centred around 3300 cm^{-1} (amide N-H stretch) and sharp peak in the range 1655-1635 cm^{-1} (C=O stretch) in all spectrums for polyamidoamine conjugates **1-5** represent the amide bond and confirmed the successful preparation of the conjugates. The presence of the amide bond also confirmed the successful incorporation of the ferrocenyl analogue, 4-ferrocenylketobutanoic acid (Fc)

in conjugates **4** and **5**. Sharp peaks corresponding to N-H bending were also observed for the carrier and the conjugates at about 1530 cm^{-1} in each spectrum. Peaks in the range of 3000-2850 cm^{-1} are attributed to C-H stretching for the alkane functional group. The peak at 1217 cm^{-1} in each spectrum of the polyamidoamine carrier and conjugates correspond to C-N stretch.

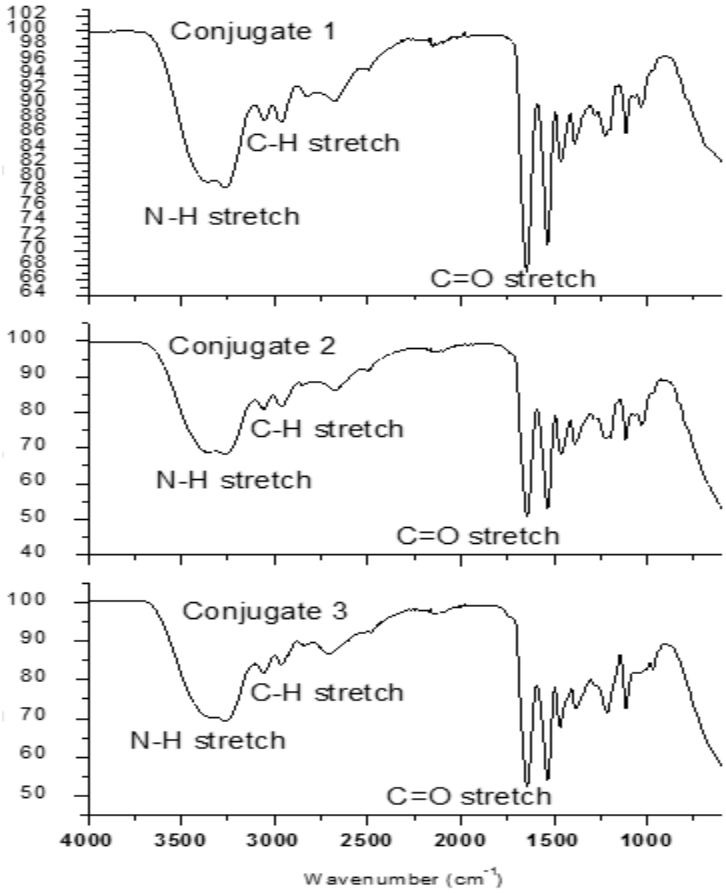

Figure 3a: FTIR spectra of conjugates **1-3**

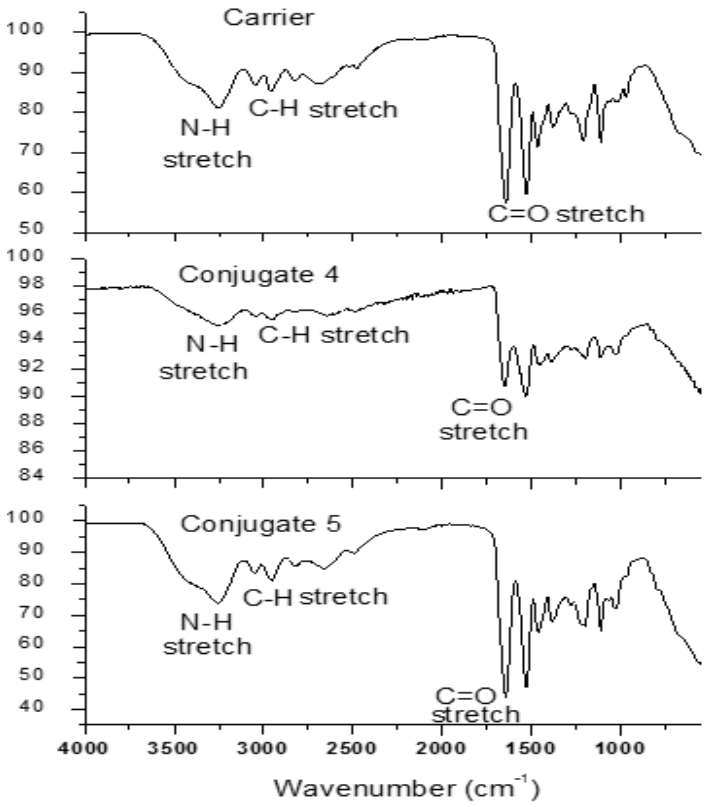

Figure 3b: FTIR spectra of the carrier and conjugates **4** and **5**

The spectrum of the polyamidoamine carrier showed a broad peak centred around 3300 cm^{-1} which represent amide N-H stretch and a sharp peak in the range 1655-1635 cm^{-1} attributed to C=O stretch confirming the successful preparation of the carrier. Peaks on the range 3000-2850 cm^{-1} are attributed to C-H stretching for alkane (**Figure 3b**).

The LC-MS further revealed fragment peaks for the polymer carriers at m/z 285, 356, 486, 569, 770, 812 and 879 confirming the successful isolation of the conjugate [**SUPP Figure 3**].

3.2. ^{1}H NMR analysis

The spectrum of conjugates and carrier showed the signal of CONH**CH_2** at about 4.40 ppm indicating the successful formation of the polyamidoamine backbone which forms the basis of the polyamidoamine carrier and conjugates (**Table 1**). The spectrum of the carrier showed signals at 1.60 ppm and 2.52-2.15 ppm which confirmed the successful incorporation of 3-dimethylamino-1-propylamine and 1,3-propanediamine, the water solubilizing *tert* amine and drug anchoring unit,

respectively into the polymer carrier backbone. The spectrum of polyamidoamine drug conjugate **1** showed signals at 0.99-0.98 ppm, 1.57 ppm and 2.69-2.33 ppm for $CH_2N(CH_2C\mathbf{H_3})_2$; $CH_2C\mathbf{H_2}CH_2N(CH_2CH_3)_2$ and $CHC\mathbf{H_2}C\mathbf{H_2}C\mathbf{H_2}C\mathbf{H_2}CH$; $C\mathbf{H_2}CH_2C\mathbf{H_2}N(\mathbf{CH_2}CH_3)_2$ indicating the presence of 3-diethylaminopropylamine and water solubilizing unit *tert* amine. Peaks at 1.57 ppm and 2.69-2.33 ppm confirm the presence of diethylenetriamine and cyclohexane-1,2-diamine dichloroplatinum(II) in the conjugate. The spectrum of conjugate **2** displayed signals for $CH_2N(CH_2C\mathbf{H_3})_2$, $CH_2C\mathbf{H_2}CH_2N(CH_2CH_3)_2$ and $C\mathbf{H_2}CH_2C\mathbf{H_2}N(\mathbf{CH_2}CH_3)_2$ at 0.86-0.83 ppm, 1.45 ppm and 2.38-2.24 ppm which confirmed the presence of 3-diethylaminopropylamine. Signals at 2.38-2.24 ppm indicate signal for $C\mathbf{H_2}C\mathbf{H_2}NHC\mathbf{H_2}C\mathbf{H_2}$ confirming the presence of diethylenetriamine and potassium tetrachloroplatinate in the conjugate. Spectrum for conjugate **3** showed peaks at 1.47 ppm and 2.31-2.03 ppm for $CH_2C\mathbf{H_2}CH_2N(CH_3)_2$, $CH_2C\mathbf{H_2}CH_2NH$ and $C\mathbf{H_2}CH_2C\mathbf{H_2}N(C\mathbf{H_3})_2$ which confirmed the presence of 3-dimethylamino-1-propylamine, 1,3-propanediamine and potassium tetrachloroplatinate in the conjugate. Spectrum of conjugate **4** showed peaks at 0.98-0.96 ppm, 1.57 ppm and 2.49-2.38 ppm for $CH_2N(CH_2\mathbf{CH_3})_2$, $CH_2C\mathbf{H_2}CH_2N(CH_2CH_3)_2$ and $C\mathbf{H_2}CH_2C\mathbf{H_2}N(C\mathbf{H_2}CH_3)_2$ signals which revealed the presence of 3-diethylaminopropylamine. Signals at 1.57 ppm, 2.49-2.38 ppm, 2.74 ppm and 4.51 ppm indicate the incorporation of the drugs; 3-[4-ferrocenylketobutamido]propylamine and potassium tetrachloroplatinate. The spectrum of conjugate **5** displayed signals at 1.18 ppm, 1.77 ppm and 2.98-2.51 ppm for $CH_2N(CH_2\mathbf{CH_3})_2$, $CHC\mathbf{H_2}C\mathbf{H_2}C\mathbf{H_2}C\mathbf{H_2}CH$ and $C\mathbf{H_2}CH_2C\mathbf{H_2}N(C\mathbf{H_2}CH_3)_2$ which showed the presence of 3-diethylaminopropylamine. On the other hand, signals at 1.77 ppm, 2.44-2.39 ppm, 2.98-2.51 ppm and 4.54 ppm also indicated the presence of 3-[4-ferrocenylketobutamido]propylamine and cyclohexane-1,2-diamine dichloroplatinum(II). The molecular weight of the repeating unit determined by H NMR was 3239.15, 3176.15, 2917.4, 3254 and 3294.9 g/mol for conjugate **1**, **2**, **3**, **4** and **5**, respectively.

Table 1: ^{1}H NMR data for polyamidoamine drug carrier and conjugates

Compound	Assignment	Chemical shift (ppm)	Proton count	
			Expected	Found
Carrier	$CH_2C\mathbf{H_2}CH_2N(CH_3)_2$, $CH_2C\mathbf{H_2}CH_2NH_2$	1.60	20	20
	$C\mathbf{H_2}CH_2CONH$, $COCH_2C\mathbf{H_2}N$, $C\mathbf{H_2}CH_2\mathbf{CH_2}N(C\mathbf{H_3})_2$, $C\mathbf{H_2}CH_2C\mathbf{H_2}NH_2$	2.52-2.15	128	140
	$CH_2C\mathbf{H_2}CONH$, $NHCOC\mathbf{H_2}CH_2$	2.72	40	47
	$CONHC\mathbf{H_2}NHCO$	4.54-4.52	20	23
Fc-PDA	$CH_2C\mathbf{H_2}CH_2NH_2$	2.75-2.73	2	2
	$CH_2CH_2C\mathbf{H_2}NH_2$	3.08-3.05	2	2
	$COC\mathbf{H_2}C\mathbf{H_2}CO$	4.22	4	5
	$CONHC\mathbf{H_2}CH_2CH_2$	4.50	2	2
	C**H** (ferrocenyl)	4.80	9	2
Conjugate 1	$CH_2N(CH_2C\mathbf{H_3})_2$	0.99-0.98	51	51
	$CH_2C\mathbf{H_2}CH_2N(CH_2CH_3)_2$, $CHC\mathbf{H_2}C\mathbf{H_2}C\mathbf{H_2}C\mathbf{H_2}CH$	1.57	29	16
	$CH_2C\mathbf{H_2}CONH$, $NHCOC\mathbf{H_2}CH_2$	2.30-2.26	40	42
	$C\mathbf{H_2}CH_2CONH$, $COCH_2C\mathbf{H_2}N$, $C\mathbf{H_2}CH_2C\mathbf{H_2}N(\mathbf{CH_2}CH_3)_2$, $C\mathbf{H_2}C\mathbf{H_2}NHC\mathbf{H_2}C\mathbf{H_2}$, $C\mathbf{H}CH_2CH_2CH_2CH_2C\mathbf{H}$	2.69-2.33	123	128
	$CONHC\mathbf{H_2}NHCO$	4.41	20	21
Conjugate 2	$CH_2N(CH_2C\mathbf{H_3})_2$	0.86-0.83	51	51
	$CH_2C\mathbf{H_2}CH_2N(CH_2CH_3)_2$	1.45	17	16
	$C\mathbf{H_2}CH_2CONH$, $COCH_2C\mathbf{H_2}N$, $C\mathbf{H_2}CH_2C\mathbf{H_2}N(\mathbf{CH_2}CH_3)_2$, $C\mathbf{H_2}C\mathbf{H_2}NHC\mathbf{H_2}C\mathbf{H_2}$	2.38-2.24	120	105
	$CH_2C\mathbf{H_2}CONH$, $NHCOC\mathbf{H_2}CH_2$	2.64-2.61	40	34
	$CONHC\mathbf{H_2}NHCO$	4.40	20	16
Conjugate 3	$CH_2C\mathbf{H_2}CH_2N(CH_3)_2$, $CH_2C\mathbf{H_2}CH_2NH$	1.47	20	20
	$C\mathbf{H_2}CH_2CONH$, $COCH_2C\mathbf{H_2}N$, $C\mathbf{H_2}CH_2C\mathbf{H_2}N(C\mathbf{H_3})_2$, $C\mathbf{H_2}CH_2C\mathbf{H_2}NH$	2.31-2.03	131	146
	$CH_2C\mathbf{H_2}CONH$, $NHCOC\mathbf{H_2}CH_2$	2.67-2.62	40	46
	$CONHC\mathbf{H_2}NHCO$	4.40	20	20
Conjugate 4	$CH_2N(CH_2\mathbf{CH_3})_2$	0.98-0.96	48	48
	$CH_2C\mathbf{H_2}CH_2N(CH_2CH_3)_2$, $CH_2C\mathbf{H_2}CH_2NH$	1.57	20	13
	$C\mathbf{H_2}CH_2CONH$, $COCH_2C\mathbf{H_2}N$, $C\mathbf{H_2}CH_2C\mathbf{H_2}N(C\mathbf{H_2}CH_3)_2$, $C\mathbf{H_2}CH_2C\mathbf{H_2}NH$	2.49-2.38	112	101
	$CH_2C\mathbf{H_2}CONH$, $NHCOC\mathbf{H_2}CH_2$, $COC\mathbf{H_2}C\mathbf{H_2}CO$	2.74	44	41
	$CONHC\mathbf{H_2}NHCO$, C**H** (ferrocenyl)	4.51	29	8
Conjugate 5	$CH_2N(CH_2\mathbf{CH_3})_2$	1.18	48	48
	$CH_2C\mathbf{H_2}CH_2N(CH_2CH_3)_2$, $CH_2C\mathbf{H_2}CH_2NH$, $CHC\mathbf{H_2}C\mathbf{H_2}C\mathbf{H_2}C\mathbf{H_2}CH$	1.77	28	16
	$CH_2C\mathbf{H_2}CONH$, $NHCOC\mathbf{H_2}CH_2$, $COC\mathbf{H_2}C\mathbf{H_2}CO$	2.44-2.39	44	42
	$C\mathbf{H_2}CH_2CONH$, $COCH_2C\mathbf{H_2}N$, $C\mathbf{H_2}CH_2C\mathbf{H_2}N(C\mathbf{H_2}CH_3)_2$, $C\mathbf{H_2}CH_2C\mathbf{H_2}NH$, $C\mathbf{H}CH_2CH_2CH_2CH_2C\mathbf{H}$	2.98-2.51	114	113.5
	$CONHC\mathbf{H_2}NHCO$, C**H** (ferrocenyl)	4.54	29	20

3.3. SEM and EDX analysis

The polyamidoamine drug conjugates and carrier were further analysed by scanning electron microscopy to study the surface morphology. **Figure 4** displays micrographs of polyamidoamine drug conjugates and carrier formed from selected amines, performed at an accelerating voltage of 15 kV and viewed at various magnifications. The carrier displayed spherical and smooth surfaces of the carrier indicating successful reaction of MBA and the amines to form the polymer. The surface morphology of the carrier and conjugate **1, 2** and **3** was smooth surfaces with swollen spherical topologies (**Figure 4a-d**). SEM image for conjugate **4** displayed flacks with rough edges morphology (**Figure 4e**) while smooth surfaced blocks topology was observed for conjugate **5** (**Figure 4f**).

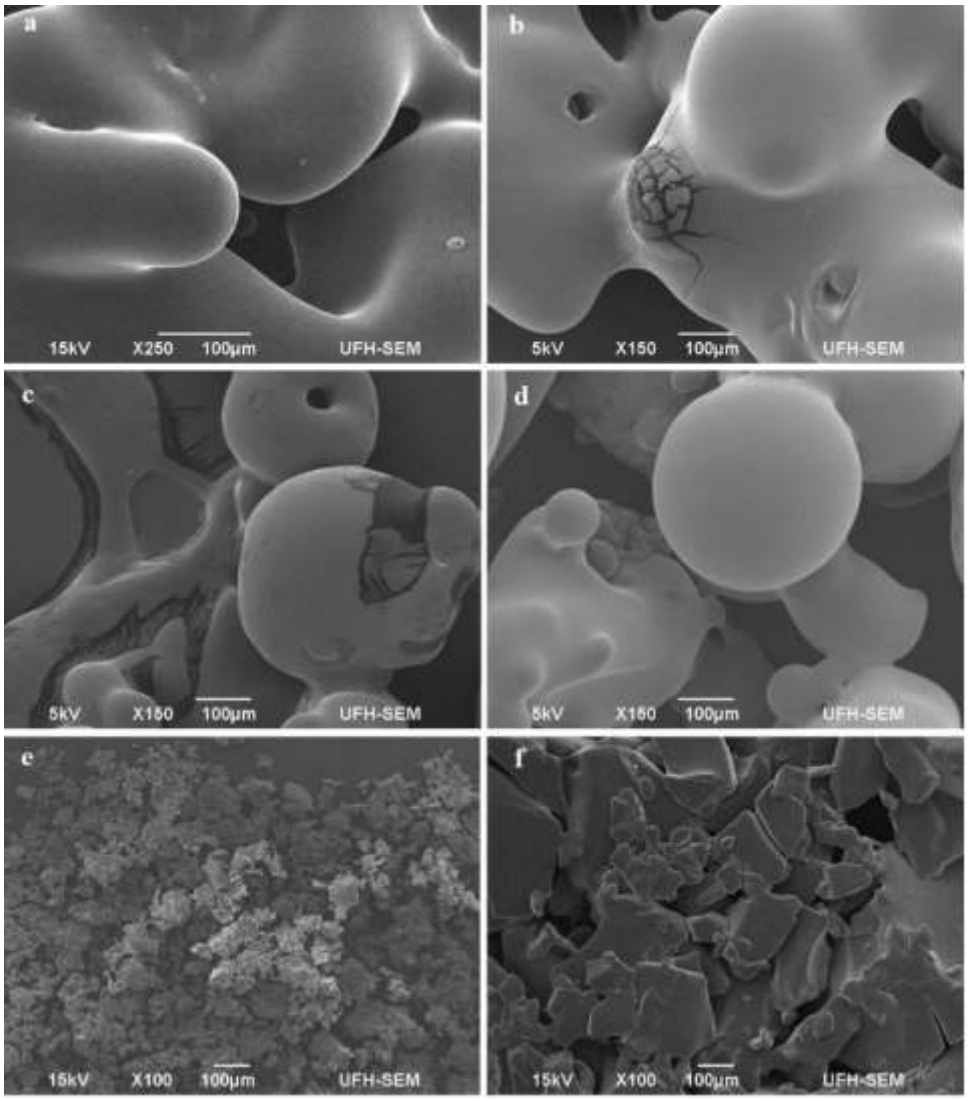

Figure 4: SEM images of (a) polyamidoamine carrier (b) conjugate **1** (c) conjugate **2** (d) conjugate **3** (e) conjugate **4** (f) conjugate **5**

EDX analysis data indicated that platinum and ferrocene-based drugs were successfully incorporated into the polyamidoamine carriers (Table 2). The platinum content in all the conjugates was in the range of 2.60–16.40% and the percentage of iron was 0.22% and 0.38% for conjugates **4** and **5**, respectively. The carbon, oxygen and nitrogen content were in the range of 25.52–47.43%, 13.32–39.0% and 3.15–18.70%, respectively.

Table 1: Weight percent composition of drug conjugates from EDX data

Conjugate	C %	N %	O %	Cl %	Pt %	Fe %
1	43.1	3.15	39.0	-	14.74	-
2	30.89	14.74	17.92	23.38	13.07	-
3	25.52	18.70	21.42	20.84	13.52	-
4	36.27	17.73	13.32	16.06	16.40	0.22
5	47.43	17.78	14.03	17.77	2.60	0.38

3.4. TEM analysis

The TEM micrographs displayed smooth spherical topologies which also correlate to spherically shaped morphology observed for surface morphology studies (SEM) of the conjugates **1-3** (**Figure 5a-c**). The sizes of the particles were obtained in the nanometre range. The TEM images also further confirmed the incorporation of platinum drug into the conjugates. The particle size of the conjugates obtained by TEM analysis was the same as the DLS analysis.

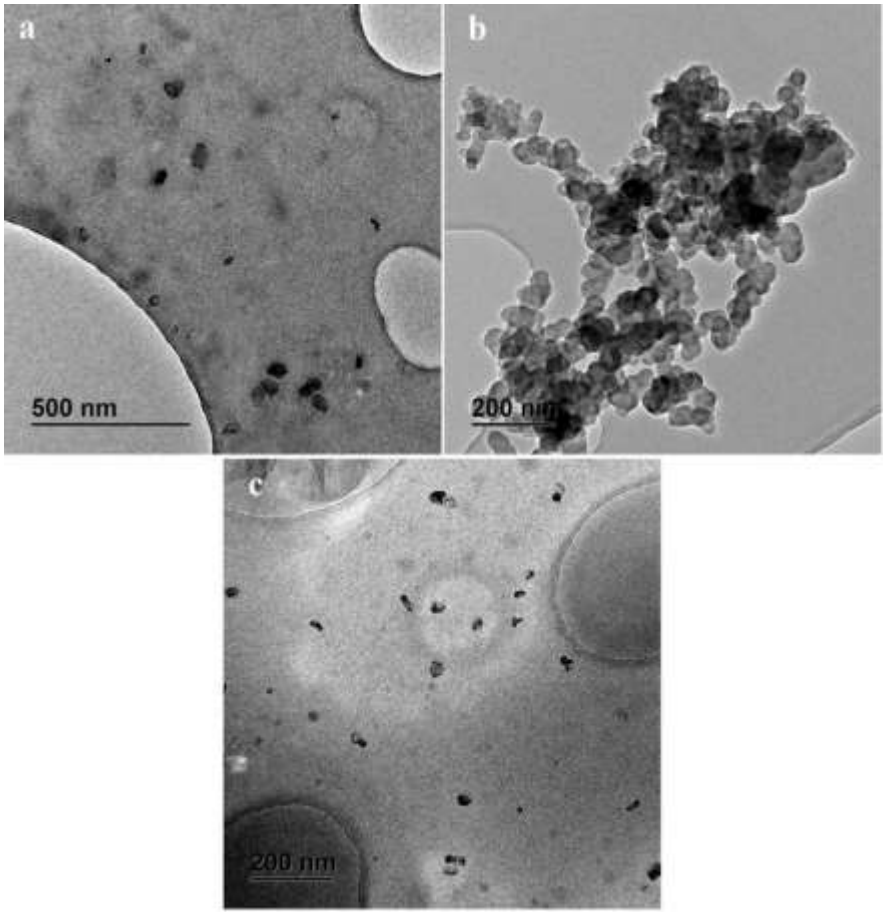

Figure 5: TEM images of (a) polyamidoamine conjugate **1** (b) conjugate **2** (c) conjugate **3**

3.5. Particle size analysis

The polyamidoamine drug conjugate particle size was 247.1 nm and 258.3 nm for conjugate **4** and **2**, respectively. The particle size of the carrier was 376.4 nm (**Table 3**). The polydispersity index (PDI) OF the conjugates increased after incorporation of the drugs into the polymer carrier. The PDI value of conjugate **2** and **4** was 0.645 and 0.439, respectively. Average particle charges was 18.1 for the carrier and 29 and 30.2 for conjugates **4** and **2**, respectively.

Table 2: Average particle size, polydispersity index (PDI) and surface charge of selected polymer drug conjugates and carrier

Compound	Average Particle Size (d.nm)	PDI (±SD)	Average Particle charge (±SD)
Carrier	376.4 ± 92.70	0.390 ± 0.057	18.1 ± 6.35
Conjugate 2	258.3 ± 46.52	0.645 ± 0.158	30.2 ± 2.15
Conjugate 4	247.1 ± 36.21	0.439 ± 0.125	29.0 ± 5.16

3.6. Drug release studies

The drug release profiles for conjugates **2** and **4**, performed at pH 1.2 and 7.4 and at a temperature of 37 °C, are provided in Figure 6. The rate of drug release was pH dependant. Platinum drug release from conjugate **2** at pH 1.2 was 51.4% after 5815 min. For the first 400 min platinum drug release from conjugate **2** was slow, however this increased in time from 1495 min to 5815 min On the other hand, platinum drug release for conjugate **2** at pH 7.4 was faster in the first 400 min where 31.6% was released in the same period. After 7300 min, 48.9% of drug was released for conjugate **2**. For conjugate **4** at pH 1.2, 16.7% of the ferrocene drug was released after 7255 min. After 7255 min, 40.7% of the platinum drug was released from conjugate **4** at pH 1.2. The percentage of ferrocene drug released was 23.4% for conjugate **4** at pH 7.4 after 7300 min whereas, 55.3% of platinum drug was released from conjugate **4** at pH 7.4 in the same time.

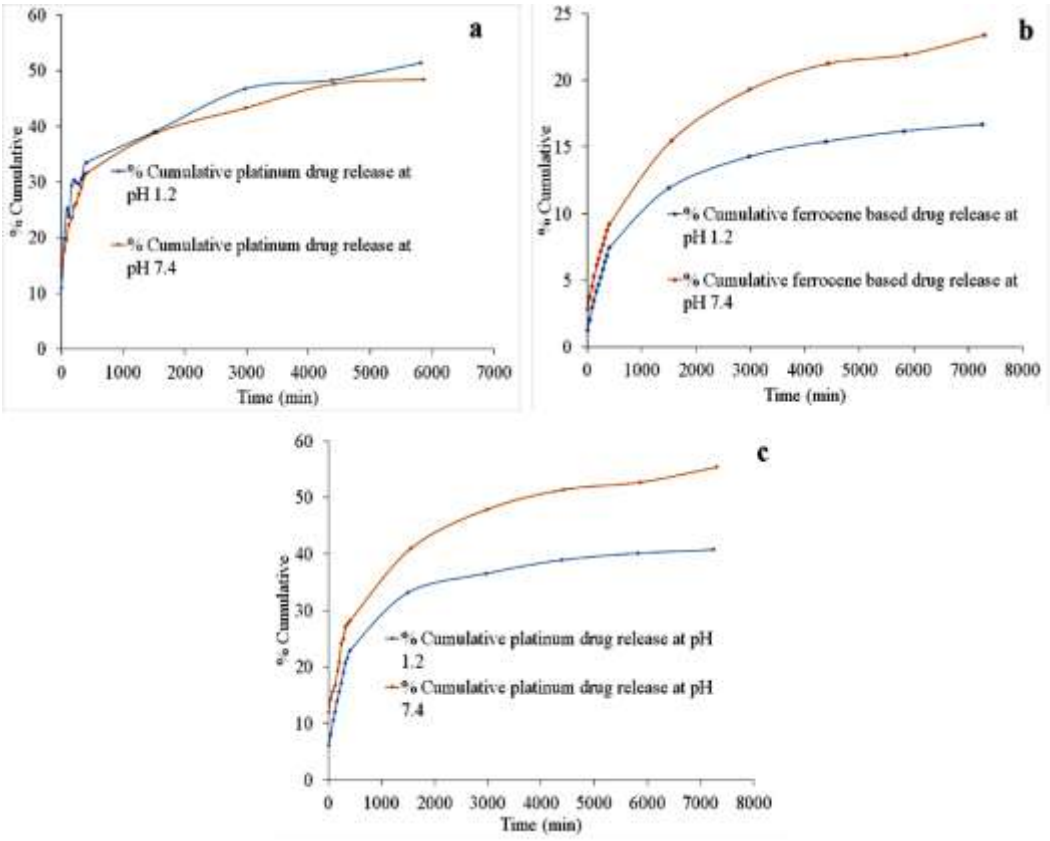

Figure 6: Percentage cumulative drug release profiles for (a) platinum drug release from conjugate **2** (b) ferrocene drug release from conjugate **4** (c) platinum drug release from conjugate **4**

3.7. Cytotoxicity activity evaluation

In vitro cytotoxicity evaluation is expressed as IC_{50}, the concentration of compound required for 50% inhibition of cell viability (Table 4). The free drugs (K_2PtCl_4 and Fc-PDA) exhibited no cytotoxic effects against all the cell lines when compared to DACH $PtCl_2$ and cisplatin, which showed good cytotoxic effects with IC_{50} values of 2.49 and 4.96 μM, respectively in MCF-7 cells (Table 4). Conjugates **1–5** and the carrier were not cytotoxic to the normal cell lines (EA.hy926), Conjugate **5** exhibited the highest cytotoxic activity against both cancer cell lines (MCF-7 and MDA-MB-231) with IC_{50} values < 1.5 μM, whereas conjugate **4** did not exhibit any cytotoxic effect. Conjugates **2** and **3** exhibited significant cytotoxic effects when compared to the free K_2PtCl_4..

Table 4: Table showing results for in vitro analysis against selected cell lines

Compound	IC_{50} ± SEM (µM)		
	MCF-7	**MDA-MB-231**	**EA.hy926**
Conjugate 1	10.68 ± 1.123	12.19 ± 1.10	88.04 ± 1.097
Conjugate 2	8.613 ± 1.179	11.48 ± 1.168	> 100
Conjugate 3	12.45 ± 1.194	13.79 ± 1.175	> 100
Conjugate 4	> 100	> 100	> 100
Conjugate 5	1.455 ± 1.260	1.468 ± 1.209	> 100
Carrier	73.01 ± 1.42	67.94 ± 1.154	> 100
K_2PtCl_4	> 100	> 100	> 100
Fc-PDA	> 100	> 100	> 100
DACH $PtCl_2$	2.49 ± 1.15	> 100	15.68 ± 1.13
Cisplatin	4.962 ± 1.267	4.124 ± 1.211	> 100

Discussion

The drug conjugates were prepared by aqueous Michael addition polymerization reaction. The reaction involved the nucleophilic addition of a nucleophile to an α,β-unsaturated carnonyl compound. The reaction is useful for the formation of C–C bond under mild reaction conditions. Additional benefits of Michael addition reactions are the accommodation of high functional groups as well as high conversions and favourable reaction rates [32]. These characteristics make the Michael addition reaction appropriate in the development of materials for biomedical applications. The carriers used provided chelating ligands for the incorporation of DACH-Pt.

The percentage platinum content was not very high, indicating the difficulty of its incorporation using non-aggressive metalation conditions. The use of an aggressive condition can result in high hydrolytic degradation leading to the loss of the structural integrity of the conjugates [33]. The incorporation of the platinum analogues into the polymer was via ethylenediamine ligands attached to the polymer backbone resulting in a structure composed of platinum tightly bound to the polymer carrier in conjugate **1** and **2** suggesting that the release of platinum would be sustained over a long period of time as it would require cleavage of the drug anchoring unit. The incorporation of platinum via an amine group ligand

in conjugates **3**, **4** and **5** suggest that the conjugates can release the incorporated platinum drug via hydrolytic cleavage of the bond connecting the platinum metal to the carrier. The second approach of the incorporation of platinum is deemed suitable for short term administration.

4-Ferrocenylketobutanoic acid was used in this study as it contains a carboxylic functional group which can be modified for conjugation into the polymer backbone. Ferrocene has been reported to result in the generation of reactive oxygen species (ROS). The reversible cellular oxidation of the ferrocenyl moiety to ferrocenium ion is accompanied by the formation of hydroxyl radicals that cause damage to the DNA [34, 35]. The unique properties of ferrocene compounds include their stability in biological media, redox activity, lipophilic nature favouring easy penetration through cell membranes, low toxicity, diversified modes of their reactions with biological substrates, as well as easiness and variability of chemical modifications and commercial availability [36]. Ferrocene is a good precursor for the development of potent anticancer compounds. It can be easily modified into compounds with good biological activity by known and simple synthetic routes. It undergoes many reactions similar to aromatic compounds making it possible to prepare substituted derivatives. It is also affordable, diamagnetic in nature, highly stable at room temperature, insensitive towards air and water, and its reversible redox characteristics make it a good starting material for the synthesis of ferrocenyl derivatives. The astounding diversity of chemistry demonstrated by ferrocene and its compounds makes it very unique when compared to other organometallic compounds [34,35,36].

The FTIR spectra of the polyamidoamine drug conjugates displayed characteristic absorption peaks at 3300 cm^{-1} for amide N–H stretch on the polymer backbone and a significant peak for C=O stretch at 1655–1635 cm^{-1} for the amide bond which confirmed the successful isolation of the conjugates (Fig. 3a, b). The presence of the amide bond also indicated the successful conjugation of 4-ferrocenylketobutanoic acid (Fc) in conjugates **4** and **5**. Similar findings have been reported by Mukaya et al. for conjugates containing ferrocene analogues [37]. The C–H stretch for the ferrocenyl ring was visible at 800 cm^{-1} confirming the successful incorporation of the ferrocene analogue in conjugates **4** and **5**. LC–MS further revealed fragment peaks for the polymer carrier backbone at m/z 285, 356, 486, 569, 770, 812 and 879, confirming the successful isolation of the conjugate (**SUPP Figure 3**).

The spectrum of the conjugates showed a signal for CONH**CH_2** at 4.40 ppm indicating the successful formation of the polyamidoamine backbone (**Table 1**). The signals for water solubilizing group in conjugate **1** were visible at 0.99-0.98 ppm, 1.57 ppm and 2.69-2.33 ppm for $CH_2N(CH_2C\mathbf{H_3})_2$; $CH_2C\mathbf{H_2}CH_2N(CH_2CH_3)_2$ and $CHC\mathbf{H_2}C\mathbf{H_2}C\mathbf{H_2}C\mathbf{H_2}CH$; $C\mathbf{H_2}CH_2C\mathbf{H_2}N(\mathbf{CH_2}CH_3)_2$. Conjugate **2-5** displayed signals for the protons on the water solubilizing groups: $CH_2N(CH_2C\mathbf{H_3})_2$, $CH_2C\mathbf{H_2}CH_2N(CH_2CH_3)_2$ and $C\mathbf{H_2}CH_2C\mathbf{H_2}N(\mathbf{CH_2}CH_3)_2$ at 0.86-0.83 ppm, 1.45 ppm and 2.38-2.24 ppm. Signals at 1.57 ppm, 2.49-2.38 ppm, 2.74 ppm and 4.51 ppm confirmed the incorporation of the drugs; 3-[4-ferrocenylketobutamido]propylamine and potassium tetrachloroplatinate. The molecular weight of the repeating unit determined by H NMR was 3239.15, 3176.15, 2917.4, 3254 and 3294.9 g/mol for conjugate **1**, **2**, **3**, **4** and **5**, respectively.

he polyamidoamine drug conjugates and carrier were further analysed by SEM to study surface morphology. The carrier displayed spherical and smooth surfaces of the carrier indicating successful reaction of MBA and the amines [17]. The surface morphology of the carrier and conjugate **1**, **2** and **3** was characterized by a smooth surface with swollen spherical topologies which can be attributed to the successful polyaddition of amines to the methylenebisacrylamide [17] (Fig. 4a–d). Similar surface morphology has been reported by Mukaya et al. [37] and Aderibigbe et al. [38]. The SEM image of conjugate **4** indicated flacks with rough edges (Fig. 4e) whereas a smooth block topology was observed for conjugate **5** (Fig. 4f). The flaked shaped and blocked shaped morphology is due to the incorporation of ferrocene derivative into the carrier. Similar morphologies have been reported [37, 39]. The percentage platinum content in the conjugates was low. SEM/EDX revealed the content of platinum in a range between 2.6 and 16.40%. The low incorporation of platinum in conjugate **5** suggest that there was a cleavage of the DACH Pt from the conjugate during the work up process, which resulted from the bulky structure of the platinum compound. The percentage of ferrocene derivative content was 0.22 and 0.38% for conjugate **4** and **5**, respectively. The low percentage of ferrocene derivative is due to strict pH of 5–6 which was employed for the conjugation of platinum into the polymer. The low % incorporation of ferrocene derivative in conjugates **4** and **5** further confirm that the acidic pH used may have resulted in the cleavage of the ferrocene derivative from the carrier backbone.

The TEM images of the conjugates displayed smooth spherical topologies (Fig. 5a–c). This provides further confirmation of the incorporation of the platinum drug into the conjugates. The particle size of the conjugates obtained by TEM analysis was similar to that obtained during DLS analysis. The polyamidoamine drug conjugate particle size was 247.1 nm and 258.3 nm for conjugate **4** and **2**, respectively. The clearance rate of nano-carriers increases with an increase in size. Nano-carriers with particle sizes between 250 nm and 3 μm have been reported to exhibit optimal in vitro phagocytosis ability, whereas those ranging between 10 and 1000 nm have been reported to be useful for biomedical applications [40, 41]. The carrier exhibited a higher particle size when compared to the drug conjugates. The PDI of the conjugates increased after the incorporation of the drugs. The PDI value of conjugates **2** and **4** was 0.645 and 0.439, respectively. The PDI values were < 1, indicating narrow molecular weight distribution and homogenous conjugation of the drug to the polymer, which favours biomedical application of the polymers because of their capability to exhibit extended residence time in the body [42, 43]. Similar findings have been reported by Patil et al. in which poly(β-L-malic acid)-doxorubicin conjugates PDI values were < 1 [44]. Also, Baumgartner et al. reported poly (l-glutamic acid) brush polymers incorporated with camptothecin with low PDI values [45]. Cao et al. also reported polymeric conjugates micelles with low PDI values, which are suggestive of a narrow molecular weight distribution [46]. The average particle charge was 18.1, 29 and 30.2 for the carrier, conjugates **4** and **2**, respectively. The high particle charge of the conjugates indicate that they are stable and have the ability to resist aggregation due to their strong repellent forces between the particles [47, 48].

Platinum drug release from conjugate **2** at pH 1.2 was 51.4% after 5815 min and at pH 7.4 48.9% after 7300 min. For conjugate **4**, 16.7% of the ferrocene drug and 40.7% of the platinum drug was released after 7255 min at pH 1.2. The percentage of ferrocene drug released was 23.4% for conjugate **4** at pH 7.4 within 7300 min and 55.3% of platinum drug under the same conditions and duration. The drug release profiles of the conjugates displayed a biphasic pattern, characterized by a general trend of fast initial release during the first 1500 min, followed by a steady and sustained release (Fig. 6). The release of platinum and ferrocene was sustained over a period of 5 days. However, the release of platinum was high compared to ferrocene, which suggests that the incorporation of the ferrocene derivative via the

amide linker slowed its release and increased its stability. Amide bonds are stable at physiological pH and are less susceptible to chemical hydrolysis [49]. The sustained release of both drugs further implies that the systems are suitable for the long term administration of drugs. Ferruti and co-workers reported similar drug release profiles for PAA-platinates at pH 5.5 and 7.4 [50]. The slow release of ferrocene and platinum from conjugate **4** (compared to conjugate **2**) may have compromised the efficacy of the drugs resulting in conjugate **4** not been cytotoxic to the cell lines tested against. More research is required to confirm this finding. Similar findings have been reported by Johnston et al. where it was found that some liposomal vincristine formulation efficacy was compromised due to the extremely slow rate of drug release [51].

The polyamidoamine carrier exhibited negligible cytotoxic activity against all cell lines confirming their low toxic profile [52, 53]. Conjugates **1**–**5** and the carrier were not cytotoxic to the normal cell line (EA.hy926), but indicated selectivity towards the breast cancer cell lines. The high cytotoxic activity of conjugate **5** against the cancer cell lines (MCF-7 and MDA-MB-231) is suggestive thereof that Fc-PDA acts as a potentiating agent when combined with DACH $PtCl_2$. The cyclohexane ring in DACH $PtCl_2$ contributes to its enhanced cytotoxic effect. The structural modification of the platinum complex influences its toxicity and activity [54]. The free drugs were inactive against the cell lines, however their inhibitory effects were noteworthy after the incorporation into the polymers. Conjugates **2** and **3** were highly cytotoxic compared to the free $KPtCl_4$. Conjugate **1** was cytotoxic to both breast cancer cell lines when compared DACH $PtCl_2$ which was not cytotxic to MDA-MB-231 cells. Similar findings have been reported by Li et al. where transplatin was found to induce cytotoxicity after incorporation into the polymers [55].

Chelation of $KPtCl_4$ with the carriers via diamine ligands resulted in cisplatin-like species. The latter most probably resulted in conjugates **1** and **3** being cytotoxic to the cancer cell lines. This has been corroborated by Neuse et al. where K_2PtCl_4 incorporation to polyaspartamide via ethylenediame resulted in conjugates with good anticancer activity [56, 57]. Conjugate **4** did not exhibit any cytotoxic effect suggesting that combining Fc-PDA with K_2PtCl_4 rather resulted in an antagonistic effect.

Conjugate **5** exhibited noteworthy cytotoxic activity when compared to the free drugs, including cisplatin.

Conclusion

Polyamidoamine carriers and conjugates incorporated with analogues of platinum and ferrocene were successfully prepared in good yields and characterized. Drug release from the conjugates was fast in the initial stage but sustained after 24 h at pH 1.2 and 7.4 and temperature of 37 °C. The polymer-drug conjugates exhibited significant cytotoxic effects when compared to the free drug. Conjugate **4** (Fc-PDA and K_2PtCl_4) was not cytotoxic to the cells suggesting that Fc-PDA produced an antagonistic effect when combined with K_2PtCl_4. However, the combination of Fc-PDA and DACH $PtCl_2$ in conjugate **5** enhanced the cytotoxicity of the drugs as observed by the IC_{50} values < 1.5 μM. Although the conjugates indicate the potential for use in the treatment of breast cancer, further research is required to confirm this.

Acknowledgments

Financial support from the Medical Research Council (Self-Initiated Research) and National Research Foundation, South Africa are gratefully acknowledged.

Conflict of interest

The authors declare no conflicts of interest.

References

1. World Health Organisation (2017) Cancer, Media Centre. http://www.who.int/mediacentre/factsheets/fs297/en/ Accessed 14 May 2017

2. H. Gheybi, H. Niknejad, A.A. Entezami. Polymer–metal complex nanoparticles-containing cisplatin and amphiphilic block copolymer for anticancer drug delivery. Des. Monomers and Polym. 17, 334-244 (2014).

3. R.P. Miller, R.K. Tadagavadi, G. Ramesh, W.B. Reeves. Mechanisms of cisplatin nephrotoxicity. Toxins (Basel) 2, 2490-2518 (2010).

4. M.A. Mashhadi, M.R. Arab, F. Azizi, M.R. Shahraki. Histological study of toxic effects of cisplatin single dose injection on rat kidney. Gene, Cell Tissue. 1, e21536 (2014).

5. S.A. Aldossary. Review on Pharmacology of Cisplatin: Clinical Use, Toxicity and Mechanism of Resistance of Cisplatin. Biomed. Pharmacol. J. 12, 7-15 (2019).

6. R. Oun, Y.E. Moussa, N.J. Wheate. The side effects of platinum-based chemotherapy drugs: a review for chemists. Dalton Trans. 47, 6645-6653 (2018).

7. G.B. Kauffman. The discovery of ferrocene, the first sandwich compound. J. Chem. Edu. 60, 185-186 (1983).

8. M. Beauperin, D. Polat, F. Roudesly, S. Top, A. Vessières, J. Oble, G. Jaouen, G. Poli. Approach to ferrocenyl-podophyllotoxin analogs and their evaluation as anti-tumor agents. J. Organomet. Chem. 839, 83-90 (2017).

9. C. Ornelas. Application of ferrocene and its derivatives in cancer research. New J. Chem. 35, 1973. (2011).

10. G. Jaouen, A. Vessières, S. Top. Ferrocifen type anticancer drugs. Chem. Soc. Rev. 44, 8802-8817 (20115).

11. R. Cavalli, A. Bisazza, R. Sessa, L. Primo, F. Fenili, A. Manfredi, E. Ranucci, P. Ferruti. Amphoteric agmatine containing polyamidoamines as carriers for plasmid DNA in vitro and in vivo delivery. Biomacromolecules. 11, 2667-2674 (2010).

12. P. Ferruti, M.A. Marchisio, R. Duncan. Poly(amido-amine)s: Biomedical applications. Macromol. Rapid. Commun. 23, 332–355 (2002).

13. P. Wu, H. Chen, R. Jin, T. Weng, J.K. Ho, C. You, L. Zhang, X. Wang, C. Han C. Non-viral gene delivery systems for tissue repair and regeneration. J. Translat Med. 16, 20 pages (2018).

14. P. Ferruti. Poly (amidoamine) s: past, present, and perspectives. J. Polym. Sci. A. 51, 2319-2353 (2013).

15. F. Martello, M. Piest, J.F. Engbersen, P. Ferruti. Effects of branched or linear architecture of

bioreducible poly (amido amine) s on their in vitro gene delivery properties. J. Control Release. 164, 372-379 (2012).

16. H.E. Mukaya, R.L. Van Zyl, N.C. Jansen van Vuuren, C.T. Chen, X.Y. Mbianda. Synthesis, characterization, biological evaluation, and drug release study of polyamidoamine-containing neridronate. Int. J. Polym. Mater. Polym. Biomater. 68, 489-498 (2018)

17. B.A. Aderibigbe, E.R. Sadiku, S.S. Ray, X.Y. Mbianda, M.C. Fotsing, S.C. Agwuncha, S.J. Owonubi. Synthesis and characterization of polyamidoamine conjugates of neridronic acid. Polym. Bull. 72, 417-439 (2015).

18. Q. Yang, R. Qi, J. Cai, X. Kang, S. Sun, H. Xiao, X. Jing, W. Li, Z. Wang. Biodegradable polymer platinum drug conjugates to overcome platinum drug resistance. RSC Adv. 5, 83343-83349 (2015).

19. V. Novohradsky, I. Zanellato, C. Marzano, J. Pracharova, J. Kasparkova, D. Gibson, V. Gandin, D. Osella, V. Brabec. Epigenetic and antitumor effects of platinum (IV)-octanoato conjugates. Sci. Rep. 7, 14 pages (2017).

20. W. Shen, J. Luan, L. Cao, J. Sun, L. Yu, J. Ding. Thermogelling polymer–platinum (IV) conjugates for long-term delivery of cisplatin. Biomacromolecules. 16, 105-115 (2014).

21. C. Zhu, J. Xiao, M. Tang, H. Feng, W. Chen, M. Du. Platinum covalent shell cross-linked micelles designed to deliver doxorubicin for synergistic combination cancer therapy. Int. J. Nanomed. 12, 3697-3710 (2017).

22. S. Aryal, C.M. Hu, V. Fu, L. Zhang. Nanoparticle drug delivery enhances the cytotoxicity of hydrophobic–hydrophilic drug conjugates. J. Mater. Chem. 22, 994-999 (2012).

23. H. Xiao, L. Yan, Y. Zhang, R. Qi, W. Li, R. Wang, S. Liu, Y. Huang, Y. Li, X. Jing. A dual-targeting hybrid platinum (IV) prodrug for enhancing efficacy. Chemical Comm. 48, 10730-10732

(2012).

24. W. Scarano, P. De Souza, M.H. Stenzel. Dual-drug delivery of curcumin and platinum drugs in polymeric micelles enhances the synergistic effects: a double act for the treatment of multidrug-resistant cancer. Biomaterials Sci. 3, 163-174 (2015).

25. K.J. Diainabo, E.W. Neuse, C.T. Chen, R. Lynne Van Zyl. Design and synthesis of polysapartamide co-drugs of platinum and methotrexate as anticancer agents. Int. J. Polym. Mater. Polym. Biomater. 68, 456-462 (2019).

26. D. Valigura, V. Vančová, G. Ondrejovič, J. Kováčová, F. Kiss. Preparation and Properties of (1, 2-Diaminocyclohexane) dichloroplatinum (II) Complexes Containing cis or trans 1, 2-Diaminocyclohexane. Collect. Czechoslov. Chem. Commun. 57, 457-462 (1992).

27 H.E. Mukaya, E.W. Neuse, R.L. van Zyl, C.T. Chen. Synthesis and preliminary bio-evaluation of polyaspartamide Co-conjugates of p-amino-salicylic acid chelated platinum (II) and ferrocene complexes. J. Inorg. Organomet. Polym. Mater. 25, 367–375 (2015).

28. W. Zhou, L. Wang, H. Yu, X. Yang, Q. Chen, J. Wang. Synthesis of a novel ferrocene-based epoxy compound and its burning rate catalytic property. RSC Adv. 6, 53679-53687 (2016).

29. A.I. Mufula, E.W. Neuse. Macromolecular carriers for methotrexate and ferrocene in cancer chemotherapy, J. Inorg. Organomet. Polym. Mater. 21, 511–526 (2011).

30. C.F. Albrecht, M.A. Stander, M.C. Grobbelaar, J. Colling, J. Kossmann, P.N. Hills, N.P. Makunga. LC–MS-based metabolomics assists with quality assessment and traceability of wild and cultivated plants of Sutherlandia frutescens (Fabaceae). S. Afr. J. Bot., 1, 33-45 (2012).

31. V. Vichai, K. Kirtikara. Sulforhodamine B colorimetric assay for cytotoxicity screening. Nat. Protoc 1, 1112-1116 (2006).

32 Hydrotrope Promoted Aza-Michael Addition Reaction. Chapter 6, pages 206-228.

https://shodhganga.inflibnet.ac.in/bitstream/10603/25448/12/12_chapter_06.pdf. Accessed 22 August 2019.

33. L.L Komane, E.H. Mukaya, E.W. Neuse, C.E. Van Rensburg. Macromolecular antiproliferative agents featuring dicarboxylato-chelated platinum. J. Inorg. Organomet. Polym. Mater. 18, 111-123 (2008).

34. S.S. Braga, A.M. Silva. A new age for iron: antitumoral ferrocenes. Organomet. 32, 5626-5639 (2013).

35. A. Vessières. Metal carbonyl tracers and the ferrocifen family: Two facets of bioorganometallic chemistry. J. Organomet. Chem. 734, 3-16 (2013).

36. V.N. Babin, Y.A. Belousov, V.I. Borisov, V.V. Gumenyuk, Y.S. Nekrasov, L.A. Ostrovskaya, I.K. Sviridova, N.S. Sergeeva, A.A. Simenel, L.V. Snegur. Ferrocenes as potential anticancer drugs. Facts and hypotheses. Russ. Chem. Bull. 63, 2405-2422 (2014).

37. E.H. Mukaya, R. Van Zyl, N.J. Van Vuuren, X.Y. Mbianda. Polymeric prodrugs containing neridronate and ferrocene: Synthesis, characterization, and antimalarial activity. Int. J. Polym. Mater. Polym. Biomater. 67, 401-409 (2018).

38. A.S. Ndamase, B.A. Aderibigbe, E.R. Sadiku, P. Labuschagne, Y. Lemmer, S.S. Ray, M. Nwamadi. Synthesis, characterization and in vitro cytotoxicity evaluation of polyamidoamine conjugate containing pamidronate and platinum drug. J. Drug Deliv. Sci. Technol. 43, 267-273 (2018).

39. B.A. Aderibigbe, S.S. Ray. Preparation, characterization and in vitro release kinetics of polyaspartamide-based conjugates containing antimalarial and anticancer agents for combination therapy. J. Drug Deliv. Sci. Technol. 36, 34-45 (2016).

40. A.K. Biswas, M.R. Islam, Z.S. Choudhury, A. Mostafa, M.F. Kadir. Nanotechnology based approaches in cancer therapeutics. Adv. Nat Sci: Nanosci. Nanotechnol. 5:043001 (2014).

41. A. Rodzinski, R. Guduru, E. Stimphil, T. Stewart, P. Liang, C. Runowicz, S. Khizroev. Targeted, controlled anticancer drug delivery and release with magnetoelectric nanoparticles, Proceedings of

the 107th Annual Meeting of the American Association for Cancer Research Apr 16-20, New Orleans, LA. Philadelphia (PA): AACR Cancer Res 76 (14 Suppl), Abstract no 2204 (2016).

42. F.M. Veronese, G. Pasut. PEGylation, successful approach to drug delivery, Drug Discov. Today 10, 1451-1458 (2005).

43. V.G. Kadajji, G.V. Betageri. Water soluble polymers for pharmaceutical applications. Polymers. 3, 1972-2009 (2011).

44. R. Patil, J. Portilla-Arias, H. Ding, B. Konda, A. Rekechenetskiy, S. Inoue, K.L. Black, E. Holler, J.Y. Ljubimova. Cellular delivery of doxorubicin via pH-controlled hydrazone linkage using multifunctional nano vehicle based on poly (β-L-malic acid). Int. J. Mol. Sci. 13, 11681-11693 (2012).

45. R. Baumgartner, D. Kuai, J. Cheng. Synthesis of controlled, high-molecular weight poly (L-glutamic acid) brush polymers, Biomater. Sci. 5, 1836-1844 (2017).

46. Y. Cao, M. Gao, C. Chen, A. Fan, J. Zhang, D. Kong, Z. Wang, D. Peer, Y. Zhao. Triggered-release polymeric conjugate micelles for on-demand intracellular drug delivery. Nanotechnology. 26, 115101 (2015).

47. S. Honary, F. Zahir. Effect of zeta potential on the properties of nano-drug delivery systems-a review (Part 2). Trop. J. Pharm. Res. 12, 265-273 (2013).

48. U. Kedar, P. Phutane, S. Shidhaye S, Kadam V. Advances in polymeric micelles for drug delivery and tumor targeting. Nanomedicine. 6, 714–729 (2010).

49. R.S. Shula, Z. Chen, K. Cheng, Strategies of drug delivery, in *Advanced Drug Delivery*, ed. by A.K. Mitra, C.H. Lee, K. Cheng (Wiley, New Jersey, 2015)

50. P. Ferruti, E. Ranucci, F. Trotta, E. Gianasi, E.G. Evagorou, Wasil M, G. Wilson, R. Duncan. Synthesis, characterisation and antitumour activity of platinum (II) complexes of novel functionalised poly(amidoamine)s, Macromol. Chem. Phys 200, 1644-1654 (1999).

51. M.J. Johnston, S.C. Semple, S.K. Klimuk, K. Edwards, M.L. Eisenhardt, E.C. Leng, G. Karlsson, D. Yanko, P.R. Cullis. Therapeutically optimized rates of drug release can be achieved by varying

the drug-to-lipid ratio in liposomal vincristine formulations. Biochim. Biophys. Acta. 1758, 55-64 (2006).

52. E. Ranucci, G. Spagnoli, P. Ferruti, D. Sgouras, R. Duncan. Poly(amidoamine)s with potential as drug carriers: degradation and cellular toxicity. J. Biomater. Sci. Polym. Ed. 2, 303-315 (1991).

53. S. Richardson, P. Ferruti P, R. Duncan. Poly(amidoamine)s as potential endosomolytic polymers: evaluation in vitro and body distribution in normal and tumour-bearing animals. J. Drug Target. 6:391-404 (1999).

54. H.S. Oberoi, N.V. Nukolova, Y. Zhao, S.M. Cohen, A.V. Kabanov, T.K. Bronich. Preparation and in vivo evaluation of dichloro (1, 2-diaminocyclohexane) platinum (II)-loaded core cross-linked polymer micelles. Chemother. Res. Pract. 10 pages (2012).

55. W. Li, M. Jiang, Y. Cao, L. Yan, R. Qi, Y. Li, X. Jing. Turning ineffective transplatin into a highly potent anticancer drug via a prodrug strategy for drug delivery and inhibiting cisplatin drug resistance. Bioconj. Chem. 27, 1802-1806 (2016).

56. E.W. Neuse, G. Caldwell, A.G. Perlwitz. Cis-diaminedichloroplatinum(II) complexes reversibly bound to water-soluble polyaspartamide carriers for chemotherapeutic applications.2. Platinum coordination to ethylenediamine ligands attached to poly(ethylene oxide)-grafted carrier polymers, J. Inorg. Organomet. Polym. 5, 195-207 (1995).

57 W.C. Shen, K. Beloussow, M.G. Meirim, E.W. Neuse, G. Caldwell. Antiproliferative activity of polymer-bound, monoamine-coordinated platinum complexes against LNCaP human metastatic prostate adenocarcinoma cells. J. Inorg. Organomet. Polym. 10, 51-60 (2000).

Supplementary material

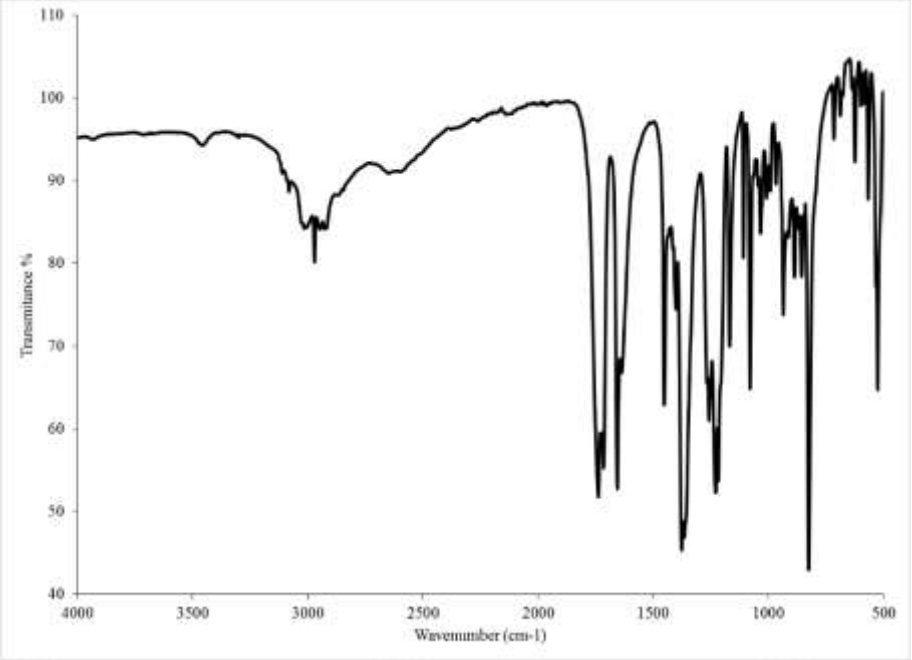

Supplementary Figure 1: FTIR spectrum of 4-Ferrocenylketobutanoic acid

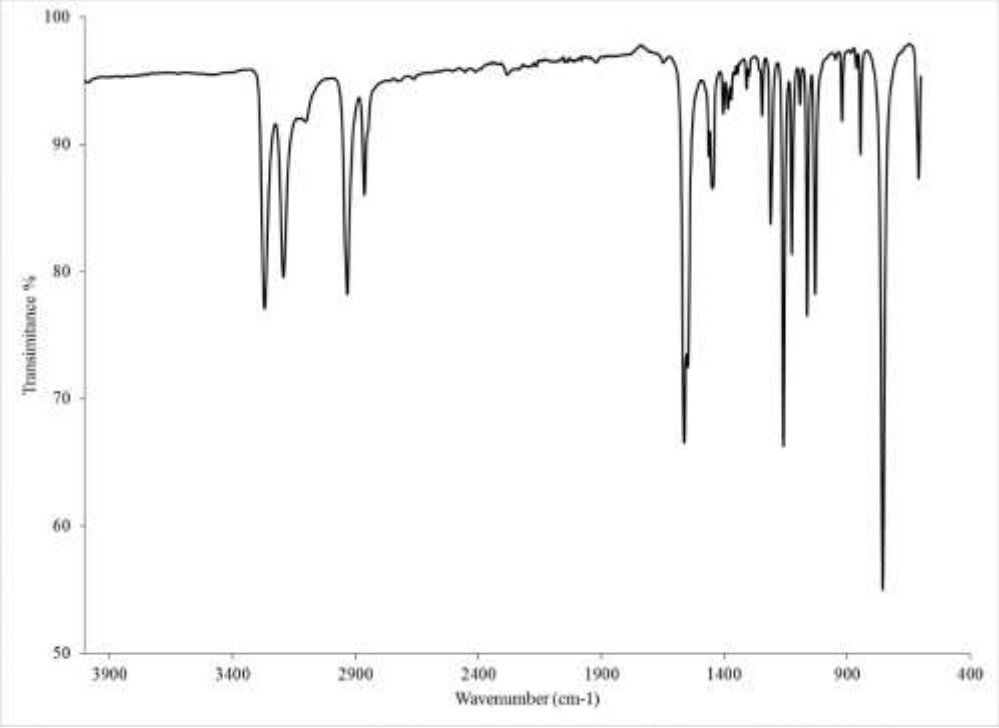

Supplementary Figure 2: FTIR spectrum of DACH-Pt

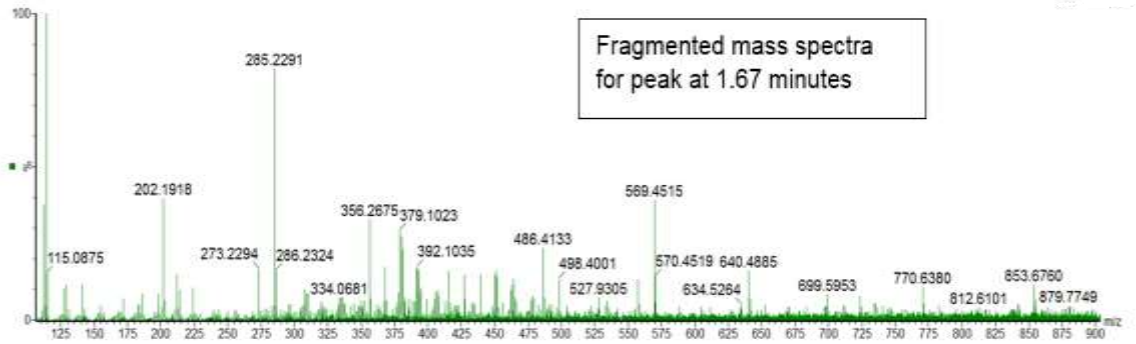

Supplementary Figure 3: LC-MS graph of conjugate **2**